Philippine Engineering Journal (1995) XVI (1): 27-48

ANALYTICAL GENERATION OF STRESS-STRAIN PROPERTIES OF COIR FIBER REINFORCED COMPOSITES IN AXIAL COMPRESSION

Pablo A. Jorillo Jr., Dr. Eng
Associate Professor

Benjamin D. Verdejo
Assistant Professor/Head

Romeo G. Lopez, Jr.
Reynaldo O. Baarde
Instructor/C.E. Specialist

Department of Civil Engineering
Integrated Research and Training Center
Technological University of the Philippines
San Marcelino, Manila

ABSTRACT

This paper examines the compressive stress-strain properties of concrete and mortar matrix reinforced with a natural cellulosic fiber i.e., coconut (coir) fiber. An extensive experimental program was carried out to investigate the inter-relationship of fiber reinforcing parameters such as fiber volume fraction, length or aspect ratio in combination with different grades of concrete or mortar matrices and the resulting stress and strain properties of the fiber-cement composite materials in axial compression. In order to characterize the stress-strain curve of a fiber concrete/mortar, a fractional second degree polynomial model developed by Sargin (1971) and modified by Wang et al. (1978) was used in this study. Findings showed that the analytical model can satisfactorily generate the complete stress-strain properties of a fiber composite material based solely on the knowledge of material properties of the composite constituents.

INTRODUCTION

In most engineering applications, material properties are best described by their stress-strain curve, which is usually based on either uniaxial compression or tension tests. For in this load-deformation relationship, it is possible to predict the ultimate behavior of a member, as well as the elastic and post-elastic characteristics specially inherent for a particular material (e.g. elastic-plastic stress-strain curve of a structural A36 stub steel column). A knowledge of the stress-strain diagram yields important information such as stress and strain range under stable and

unstable conditions, and the shape of the ascending and descending curve as well as the area under the descending portion which is a qualitative measure of toughness and energy absorbing capability of a material.

Previous works have indicated that the ductility, toughness, resistance to impact, and improvement of post-cracking characteristics of a cement-based material such as concrete or mortar can be greatly improved through the inclusion of short randomly oriented fiber (Wang et al., 1978, Fanella et al., 1985, Swamy, 1981, Jorillo, 1992). However, only high modulus fibers such as steel and glass fibers *(E = 70-220 GPa)* are capable of imparting significant increase to the compressive strength of the composite. Low elastic modulus fibers ***(E = 0.5 - 50 GPa)*** such as polypropylene, nylon and natural cellulosic fibers, on the other hand, are not capable of producing strong composites with high strength, although other merits such as quasi-ductile and large energy absorption capabilities can be imparted by these types of fibers to the composite aside from this "*increase-in-strength*" merit (Jorillo, 1991, Gram 1984, Swamy 1990). This ductile property of fiber-cement composite is best manifested by its load-deformation response curve.

Composites reinforced with natural fibers have special relevance to developing countries in view of their low cost, ready availability, savings in energy and their ready application to the rapid development of the country's infrastructure. Studies by Jorillo (1994) Jorillo and Suzuki (1994) and Hussin (1993) have shown that natural fibers in gypsum or cement matrix in form of full-scale pre-cast elements can exhibit strength and ductility characteristic comparable to that reinforced with synthetic and more expensive polypropylene or nylon fibers. Hence, deeper investigation of the effect of natural cellulosic fiber such as coconut (coir) fiber to the resulting stress and strain properties of the composite will enable the understanding on how low modulus fiber reinforced a cement-based matrix under axial compression.

It is the objective of this study to comprehensively evaluate the stress and strain properties of coir fiber composite. Correlation of the pertinent relationships between the fibers parameters in combination with matrix properties and resulting compression properties, through the analytical generation of the entire stress-strain diagram based from the given material properties is the primary aim of this study.

THEORETICAL BACKGROUND

Due to the advent of non-linear analysis of reinforced and prestressed concrete structures, knowledge of the complete force-deformation relationship of section became necessary. Popovics (1973) cited some important advantages on the knowledge of the stress-strain diagram:

a. entire deformation history may provide indirect information concerning internal structure as well as the failure mechanism of a material and its constituents,
b. it enables to compute deflections,
c. compute stresses from observed strains,
d. loss of prestress in a prestressed concrete, and so forth.

Generally, the stres-strain of concrete in compression is defined as:

$$\sigma = f(\varepsilon, A, B, C, D, \ldots, Z) \qquad (1)$$

where σ is the stress in concrete with its corresponding strain ϵ, and the constants A, B, D,...,Z are various parameters that affect the behavior of the material. As early as 1950, Hognestad (1955) developed a simplified stress-strain model of a second degree parabola and a straight line, with an objective of deriving a better and more general stress block for concrete design and analysis. In 1960 Kriz and Lee (1960) used a second degree polynomial form wherein the concrete parameters were determined from Hognestad's experiment. Work of Rushch (19), Saenz (1961), Dezaji and Krishnan (1969) and among others were reviewed by Sargin (1971) in his works published in the University of Waterloo. Sargin (1971) himself proposed a fractional equation of second order polynomial in a non-dimensional form,

$$Y = k\frac{A + Bx + Cx^2}{I + Dx + Ex^2} \qquad (2)$$

where the normalized stress $Y = \sigma/\sigma_p$. The normalized strain is given as $x = \epsilon/\epsilon_p$, and k, A, B, C, D and E are constants which can be derived from the boundary conditions and material properties. Also the suffixes p, i, and l refer to the peak, inflection and last point in the stress-deformation diagram. Careirra and Chu (1985) noted that in choosing for an analytical model for the stress-strain relationship of concrete in compression, the following should be taken into consideration:

a. the parameters that defined the relationship are physically significant and can be estimated from simple empirical relationships.
b. ascending and descending branch shall be shown, and
c. equation is simple and should compare favorably with the experimental data.

From these criteria, a fractional equation of second order proposed by Sargin (1971) and modified by Wang et al. (1978) and later used by Fanella et al.(1985) in application to steel fiber concrete was adopted in this study. It is given in non-dimensional form of

$$Y = \frac{Ax + Bx^2}{I + Cx + Dx^2} \qquad (3)$$

where *Y and X* are normalize stress and strain. The constants A, B, C and D can be likewise derived from the boundary conditions and the material properties. A different set of constants

are applied for both ascending and descending portion of the curve, and these are calculated based on two sets of four boundary conditions shown in Table 1. Figure 1 shows this relationship schematically.

Table 1
Boundary Condition for the Stress-strain Expression

Ascending Portion	Descending Portion
1. $dy/dx = A$	1. $Y = 1.00$, $X = 1.00$, $dy/dx = 0$
2. curve passes at $Y = 0.45$, $X = 0.45$	2. curve passes inflection point $x = \varepsilon_1/\varepsilon_p$, $Y = \sigma_1/\sigma_p$
3. curve passes at $Y = 1.00$, $X = 1.00$	3. passes inflection point $d^2y/dx^2 = 0$
4. curve passes at $Y = 1.00$, $X = 1.00$	4. passes last reference point $x = \varepsilon_1/\varepsilon_p$, $Y = \sigma_1/\sigma_p$

From the boundary condition, the constants *A, B, C* and *D* can be expressed in terms of physically significant parameters in the stress-strain curve like σ_p, ϵ_p, σ_i, ϵ_i, σ_l and so on. If these stress-strain parameters are expressed in terms of available material properties such as matrix compressive strength (σm) and amount of confinement offered by the reinforcing fiber *(Vf, lf/d)* the analytical generation of the entire stress-strain curve can be easily facilitated.

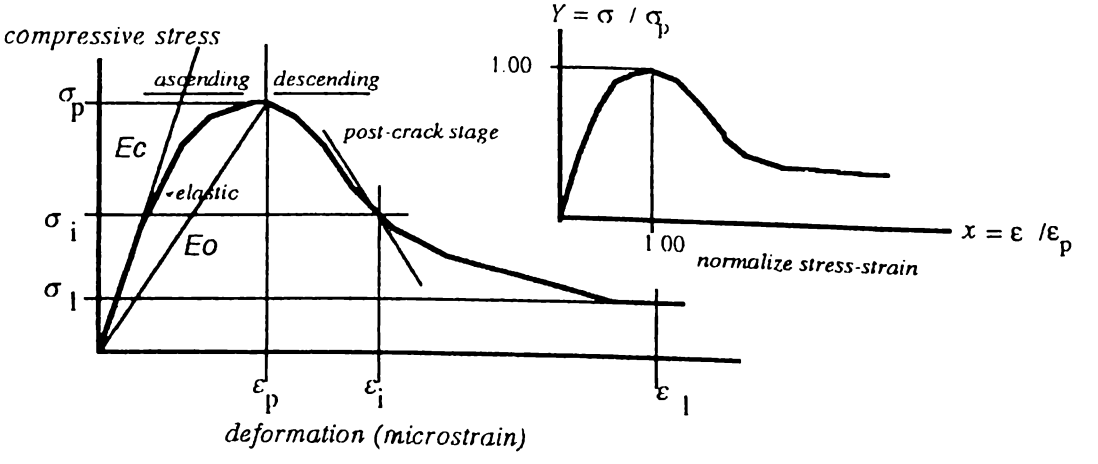

Figure 1
Schematic Diagram of the Stress-strain

EXPERIMENTAL PROGRAM

An extensive experimental program was carried out to determine the influence of fiber reinforcing parameters such as fiber volume fraction (Vf), and aspect ratio (l/d) in combination with different grades of concrete / mortar matrices to the compressive stress-strain properties of coir fiber cement composite. Stress-strain properties refer to the characteristics of peak stress and strain *(σp, cp)*, secant and tangential modulus *(Ec, Eo)*, inflection stress and strain *(σi, ci)*, and residual stress *(σl)* at last strain of 12,000 μc. The test detail for both fiber-mortar and fiber-concrete are shown in Table 2. Note the mix code designation for concrete and mortar-based composite in Table 5, e.g. for concrete with *W/C = 60%* and reinforced with 30 mm fiber, a code of 3C60 was used.

Table 2
Variables considered in the test program

Water-Cement % (W/C)	Fiber Volume % (Vf)	Mix Proportion C:S:G	Limitation and Fresh Properties
40	0 0.5 1.0 2.0 3.0	1: 2.7: 1.8 1: 2.0: 1.5 1: 1.8: 1.4 1: 1.2: 1.0 1: 1.3: 0.8	lf = 30 mm Υ = 2150-2350 kg/m^3 Air = 3.5 - 4.1 % Slump = 12.0 (ave.) Cement Content = 500 kg/m^3 (ave.)
50	0 0.5 1.0 2.0 3.0	1: 2.7: 1.9 1: 2.3: 1.5 1: 2.2: 1.4 1: 1.4: 1.0 1: 1.3: 0.8	lf = 15, 30, 50 mm Υ = 2020-2370 kg/m^3 Air = 3.5 - 4.2 % Slump = 12.0 (ave.) Cement Content = 450 kg/m^3 (ave.)
60	0 0.5 1.0 2.0 3.0	1: 3.9: 2.6 1: 3.1: 2.1 1: 3.0: 2.0 1: 2.3: 1.3 1: 2.3: 1.2	lf = 30 mm Υ = 2050-2200 kg/m^3 Air = 4.1 - 5.4 % Slump = 14.0 (ave.) Cement Content = 360 kg/m^3 (ave.)
40	0.40	1: 1.0: 0.0	Flow = 150-211 mm mortar mixture
50	0.40	1: 2.0: 0.0	Flow = 130-200 mm mortar mixture
60	0.40	1: 3.0: 0.0	Flow = 130-200 mm mortar mixture

Materials and Sample Preparation

ASTM Type-1 Portland cement with specific gravity of 3.15 was used as the binding medium. An ordinary river sand with a maximum size of 2.5 mm. specifying gravity of 2.55, and absorption of 1.25% was used as fine aggregates. For the coarse aggregates, a river gravel of max. size of 20 mm, specific gravity of 2.62, fineness modulus of 6.26, and absorption of 2.4% was used.

Coconut fibers *(Cocos Nicifera Linn.)* derived from an air-dried coconut husk harvested for copra were used as the natural cellulosic fiber. Fiber preparation was described in detail elsewhere (Schaffiner, 1988). Saturated surface dry fibers were cut to three different length groups, namely, 30, 60 and 90 mm with equivalent aspect ratio (l/d) of approximately 100, 200, and 300, respectively. The fibers were uniformly dispersed in a plastic consistent mortar while mixing.

The constituent materials were mixed in a forced-mixing type pan mixer in the following order: (1) half of the dry materials and three-fourths water, (2) gradual dispersion of half the volume of fiber, (3) addition of remaining water and fibers, and (4) two minutes final mixing. Specimens were cast into reusable steel molds and were vibrated externally. After 24 hours, the specimen were stored in 25°C water for the curing ages of 7 and 28 days.

Test Methods

Properties in compression was obtained from the testing of 100 ϕ x 200 mm cylinder. All specimens were cement capped as per ASTM and tested in a 200T hydraulic Universal Testing Machine at a constant stress rate of 300 kgf/cm^2/min. A deformation measurement apparatus (Figure 1) was set in accordance with JIS SF-5 (1984) in order to measure the stress-strain diagram of various fiber-concrete/mortar specimen. Strains were measured at middle third height of the cylinder by two linear variable differential transducers (LVDT). and was directly plotted in conjunction with applied load in the X-Y recorder.

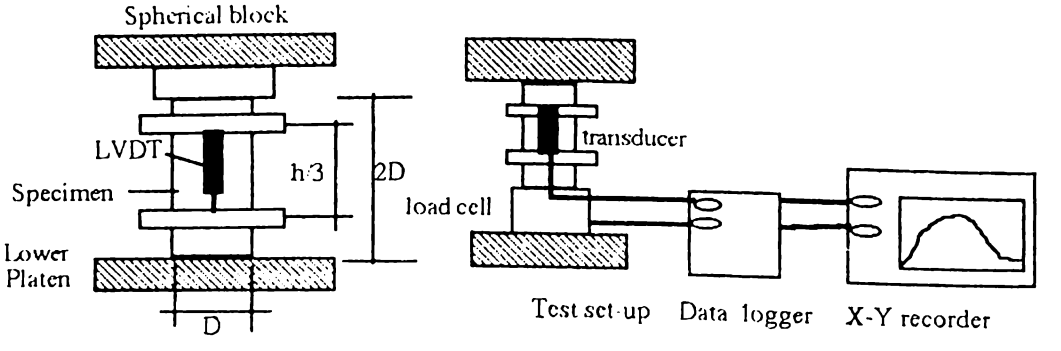

Figure 2
Compression Test Set-up and Measurement System

RESULTS AND DISCUSSION

Structural integrity of the brittle matrix was greatly enhanced due to the reinforcement of coconut husk (coir) fibers. During the compression test it was observed that the failure of the specimen was gradual, in spite of the presence of excessive vertical cracks. The occurrence of the shallow slope in the descending portion of the stress-strain curve confirmed this behavior. The presence of fiber altered the basic characteristics of the stress-strain curve. While the ascending portion of the curve was only slightly altered, the descending portion was greatly improved. The following points were observed from the typical experimental stress-strain diagram for both mortar and concrete based composite:

a. slight changes in the elastic slope
b. farther location of strain (i.e. larger strain) at ultimate stress,
c. shallow slope in the post-crack portion, and
d. increased overall area under the curve

Furthermore, differences in the stress-strain characteristics between a mortar and a gravel-concrete based fiber composite having essentially the same strengths was also seen. The mortar-based composite exhibits a smaller secant modulus of elasticity (E), larger peak strain (ϵ_p) and a steeper drop in the descending part of the stress-strain curve compared to the gravel-concrete based. This means that if an analytical stress-strain is expressed as a function of the matrix compressive strength and fiber parameters alone, a separate equation would be required for each type of matrix that is one for the concrete based and another for a mortar-based. Although a more general equation which can be applied for both types of matrices is desirable, in this study separate analytic expressions were opted because of the limited range of matrix parameters (e.g. sand-aggregate ratio S/A, aggregate/cement ratio A/C, grading and maximum size of coarse aggregates, etc.) that were chosen in the test program.

The observed properties as listed in Table 3 were correlated with fiber reinforcing parameters (Vf, lf, l/d) and base matrix properties (σ_m, E_m) in order to derive a simple prediction equations which can be used in calculating the basic compressive properties, and in turn, in the analytical generation of the entire stress-strain diagram. In the statistical analysis of data, several combinations of the independent variables (e.g. Vf, Vf(l/d), Vf/σ_c, etc.) were examined to improve the correlation of the observed data and the prediction equation. Although non-linear expressions can be derived, square-fitting lines were used for simplicity. For every dependent variable y, such as compressive strength, the following prediction equation was sought

$$y = a + bx \qquad (4)$$

where x is an independent variable and a and b are the parameters (intercept and slope) of the regression equation. Several values of the independent variable x were tried to improve the correlation between the data and predicted line. However, a criteria that the relationship must be physically significant and theoretically correct was enforced in order to make sure that the correlation of the two variables are physically valid.

Ultimate Compressive Strength

A typical trend for general fiber concrete such as aramid (Ward and Lee, 1990), steel (Walkus et al.., 1979), pan-based carbon (Akihama, et al.., 1986), and polypropylene fibers (Dardare, 1980) can also be seen in the case of coir fiber cement composite, that is, the effect of fiber addition to compressive strength at low volume fraction is negligible (Figure 3). This is evident in both mortar and concrete-based composite. Variation in strengths at Vf range of 0.5 to 2.0% is about 12% only. However, fiber addition in excess of 2.0% caused a marked decrease in the compressive strength. This may be due to increase porosity brought about by the presence of fiber balls or by ineffective compaction of the high Vf mixture. Furthermore, at high Vf content it was necessary to reduce the proportions of the aggregates to meet the workability requirement. This may have consequently resulted to a weakening of the fiber-matrix bond due to the lack of sufficient matrix necessary for efficient fiber embedment. This observed trend is not unique for coir fiber composite only but to all FRC materials in general, may it be a high modulus fiber or a low modulus fiber cement composite.

In Figure 3(c), it is clear that no unique relationship exist between fiber length *(lf)* and the compressive properties (i.e. ultimate strength σ_c, secant modulus of elasticity *Ec*, and peak strain ϵp) at all fiber volume levels. Variation in the strength, elastic modulus, and the peak strain at fiber lengths of 15, 30, and 50mm are about 10% only can be considered negligible. Also, a very low correlation factor exist between compressive properties and fiber lengths confirming the absence of any direct relationship.

The compressive strength of the composite was correlated to the matrix and fiber parameters in the ***Law of Mixture*** form of σ_c-$\sigma_m(l\ Vf) + \sigma fVf$, that is, the strength of the composite is a contribution of matrix (σ_m) and fiber reinforcement (*Vf*). The prediction equation for mortar and concrete-based composite with a coefficient of correlation (r) of 0.9821 and 0.9751 respectively (Figure 4), are given as

$$\text{concrete:}\quad \sigma_c = 1.0685\ \sigma_m(1-Vf) - 1216\ Vf \tag{5a}$$

$$\text{mortar :}\quad \sigma_c = 0.9802\ \sigma_m(1-Vf) - 1726\ Vf \tag{5b}$$

where the compressive strength of composite (σ_c), and matrix (σ_m) are in kgf/cm^2. Fiber volume fraction, *Vf* in 1/100%. The negative constants - 1216 and - 1726 indicate the general trend observed in the experimental results, i.e., decrease in strength for an increasing fiber volume. A separate equation was provided for mortar and concrete-based composite, for the reason that these materials exhibited an entirely different stress-strain characteristics. Also, the range of variables chosen such as *S/C, A/C, and W/C* is not comprehensive enough to generalize the key characteristics of the stress-strain diagram into a single equation that would be applicable for both mortar and concrete. Hence, separate equations were presented here.

Secant Modulus of Elasticity

The secant modulus of elasticity (*Ec*) was obtained at 45% of the ultimate compressive strength. It can be observed in Figure 5 that for fiber content of up to 1.0% the effect to the

elastic modulus is negligible. However, a decrease in elastic modulus occurred for fiber volume inclusion in excess of 2.0%. Although there are many factors which cause such behavior, it is believed that the porosity of the material brought about by fiber balling and ineffective compaction is the major cause of this reduction. Comparison of the data with the established American Concrete Institute (ACI, 1989) and Japan Concrete Institute (JCI, 1985) equation for the same range of unit weight (γ), revealed a 15-20% less elastic modulus. As an upper limit, the elastic modulus of fiber concrete with Vf = 0.5-2.0% can be seen to be approximately 0.85% of base matrix modulus (Em). The reason for this slight decrease is presumed to be due to the following factors:

a. increased porosity brought about by the interwined fiber which entrapped more air and inhibited the effective compaction of the mixture during casting.
b. increase local stress and strain concentration due to elasticity mismatch, that is, relative weakness between cement paste, aggregates and fibers, and
c. inherent low modulus and high poison ratio of the fibers.

As for the effect of length, it was found that the secant modulus of elasticity is practically independent of the fiber length or aspect ratio. The differences found in the values of the elastic modulus at different lengths can be attributed to the normal scatter or to the inherent variability of modulus of elasticity of concrete. Hence the prediction equation are expressed in terms of fiber volume and matrix compressive strength only. It is derived and given as.

$$\text{concrete:} \quad E_c = 803.6\ \sigma_m + 860.940\ Vf \qquad (6a)$$

$$\text{mortar:} \quad E_c = 587.8\ \sigma_m + 448.790\ Vf \qquad (6b)$$

where ***Ec*** is the secant modulus of elasticity in kgf/cm^2. Note that the equation also reflects the observation seen in the experimental stress-strain diagrams, that is, the elastic modulus of mortar is less than that of concrete due to the absence of high modulus coarse aggregates. Equations 6 can be used as a first hand approximation of the elastic modulus for compressive strengths ***(σc)*** range of 200-500 kgf/cm^2.

Peak Compressive Strain

Despite of no improvement found in the compressive strength and elastic modulus, modest enhancements in peak strain occurred due to the inclusion of fibers. Increasing matrix strength and fiber content resulted to an increase in peak strain ranging from 15 to 30%. Figure 7 illustrates the significant effect of fiber volume to this increase in strain. Measured peak strain of 2500-3500 $\mu\epsilon$ was observed for composite with ***Vf = 2.0%*** compared to the 1500-2000 $\mu\epsilon$ for base concrete. Results of Gopalaratnam and Shah (1987) on steel fiber concrete with fiber volume fraction of 1.0-2.0% showed that the maximum strain of the FRC is 3125-3550 $\mu\epsilon$ while the plain concrete is at 1800-1900 $\mu\epsilon$. This indicate the comparable increase in strain capacity of coir fiber concrete. This property entails higher degree of toughness due to the increased area under stress-strain diagram. Although the exact mechanism of failure of fiber and matrix in compression is not clearly known, improvement in peak strain may be brought by the presence of

fibers which offered an additional confinement to concrete. This may have controlled the lateral expansion, which in turn, enabled the material to carry an additional longitudinal strain beyond the limit which a base matrix can carry alone. Assuming that the strains measured by the pair of transducent (LVDT) at the middle third height gives a valid material response, the prediction equation for peak strain in terms of fiber volume and composite strength are given.

$$\text{concrete:}\quad \epsilon p = 45{,}890\ Vf + 4.78\sigma c \qquad (7a)$$

$$\text{mortar:}\quad \epsilon p = 52{,}682\ Vf + 6.19\sigma c \qquad (7b)$$

where ϵp is the peak strain in compression given in $\mu\epsilon$. Figure 8 illustrates the correlation of this stress-strain parameter with matrix and fiber parameters. The higher peak strain observed for mortar can be attributed to the absence of stiff coarse aggregates which presumably allowed the matrix to deform further. Also it is possible that the confining effect of fiber is more effective with a more homogeneous matrix like the mortar.

The values of the peak strain obtained here are basically of the same order as that reported by Hognestad et al.(1955) and Gopalaratnam et al.(1987). However, it is lower by the order of 500-1000 $\mu\epsilon$ than those reported by Fanella et al. (1985) and Wang et al. (1978) in their work with steel and monofilament and twisted polypropylene fibers, respectively. The difference may be attributed to the material and specimen type, method of testing, and conditions of test. It should be noted that in this experiment, a constant load rate application in a stiff testing machine 2.0 MN (200T) was used instead of the closed loop constant strain rate method.

Post-Crack Properties

All other characteristics parameters such as stress and strain at inflection point $(\sigma i,\ \epsilon i)$ and arbitrary last point $(\sigma l\ \epsilon l)$ were likewise correlated with the matrix and reinforcing parameters and summarized in Table 3 for mortar and concrete-based composite. The stress-strain at the inflection point were graphically located as the point of curve deviation from its regular parabolic shape or point of curvature deviation mathematically represented as d^2y/dx^2. The final far point in the stress and strain curve was arbitrarily set at $12{,}000\ \mu\epsilon$, and its corresponding stress (σl) was also graphically measured.

Also shown in Table 3 are the statistical characteristics of the data including the correlation coefficient and the coefficient of variations, which indicate how well data are approximated by a straight line. As to the form of equations in Table 4 the following remarks are in order.

a. As observed from the trend and correlation of strains $(\epsilon_p,\ \epsilon_i,\ and\ \epsilon_l)$ with fiber length (lf), no unique relationship exist between the two variables, and hence the form $\epsilon = a\sigma_c + bVf$ was adopted.
b. Coefficient of variation (CV) was computed using equations 8 and 9. The low values of CV and correlation coefficient for strain ϵ_i *and* ϵ_l can be attributed to the observed wide scatter of these strains. This is due to the various mode of failure of the cylinder specimen which can be significantly affected by its matrix strength, stiffness, and amount of confining material.

Table 3
Summary of the Prediction Equation of the Keypoint of Stress-strain Curve

Matrix Type	y	a	bx	Correlation Coefficient, r	Coeff of variation, w (%)
Concrete	σc	1726 Vf	0.98 σm(l Vf)	0.982	14.5
	Ec	44.8E04 Vf	587.5σm	0.972	16.4
	εp	52.6E03 Vf	6.19 σc	0.931	23.8
	εi	12.3E03 Vf	6.87 σc	0.762	40.9
	σi	304.1 Vf	0.72 σc	0.975	17.7
	σl	1721 Vf	0.13 σc	0.879	28.9
Mortar	σc	1216 Vf	1.068 σm(l Vf)	0.975	14.6
	Ec	86.1E04 Vf	803.6 σm	0.959	17.6
	εp	45.9E04 Vf	4.78 σc	0.881	28.6
	εi	10.5E04 Vf	6.64 σc	0.766	40.3
	σi	1150 Vf	0.69 σc	0.917	25.5
	σl	2588 Vf	0.16 σc	0.695	45.3

Analytical Modeling of Stress-strain curve

The modified analytical expression first developed by Sargin (1971) for uniaxial compression of concrete was used in this study. The same model was used for both ascending and descending branches of the curve, but of different set of constants A, B, C and D. These constants were determined from the boundary conditions described by Fanella (1985), Wang (1978), and Sargin (1971), and summarized in Table 4.

Table 4
Computation of the Analytical Stress-strain Constant

Ascending	Descending
Al = Ec/Eo Bl = Dl - 1 Cl = Al -2 Dl = Al' = (bl'/Cl') where: Al' = 2.22 Al^2 Bl' = 0.45 (0.41/Al) + (0.2/Al^2) Cl' = 0.11/Al^2 Ec = Secant modulus of elasticity Eo = σc/εp (tangential modulus of elasticity) σi, εi = inflection point of stress and strain σf, εf = last/final point of stress and strain	A2 = A2'/B2' B2 = D2 - 1 C2 = A2 -2 D2 = A2"/B2' where: A2' = cl b2 -c2bl A2" = al c2 -a2 cl B2' = alb2-a2bl al = εi - εiσi a2 = εf - εfσf b1 = $εi^2$-$εi^2$σi b2 = $εf^2$- $εf^2$σf c1 = σi -2 εiσi + $εI^2$ c2 = σf - 2εfσf + $εf^2$

Substitution of volume fractions and properties of matrix and fiber into the prediction equations in Table 3 will yield the key points of the compressive stress-strain diagram. In turn these values when substituted to Table 4 will generate the coordinates of the keypoints necessary in the computation of the constants of the analytical model. A straight forward flow chart of the entire process is given in Figure 9. Based on these, a compute program was written to generate the analytic stress-strain. The program first calculates the coordinate of four keypoints based from the given material properties. Then the constants A,B,C, and D are calculated separately for the ascending and descending portion of the curve. Finally the non-dimensional and dimensional analytic curve are plotted.

The experimental stress-strain curve of 3 to 5 specimens were averaged and compared to the analytical curve generated for a compressive strength equal to the averaged matrix strength, see Figure 10. A comparison of the observed and the analytical generated curve shows good correlation. Good fit occurred for almost all specimens under the elastic or the ascending curve, while a slight offset occurred under the post cracking portion or the descending portion of the curve. This can be explained from the wide variation of the values of the stress and strains at inflection point (σ_i, ϵ_i) and at the last point (σ_l) compared to the key points in the ascending stage of the stress-strain.

The analytical curve shows trends similar to the experimental data. The statistical variation of the observed and the analytical curve was computed using Eqs. 8 and 9, and was found to be in the range of 8.0% to 20% which is very satisfactory. the representation of the precision of prediction results for every N set of data is written as

$$\omega = \frac{1}{\mu_j}\left(\frac{1}{n-1}\sum_{i=1}^{n}\mu_{ij}^{\ 2}\right)^2 \tag{8}$$

$$\mu_j = 1/n\sum_{i=1}^{n}\xi_{ij} \tag{9}$$

where ij(i=1,2,..,n, j=1,2,..,N) are the test data, n is the number of data, N is the number of data set, j represents the jth set of experiments, i represents the ith datum in the jth set of experiment, μij is the error between experiment and prediction result, μj is the average value of the jth set of experiment.

Caution should be taken in extrapolating the material properties beyond the limited chosen variables of Vf=0.5-4.0%, lf=10-60mm, σ_m=200-500 kgf/cm^2, because it may show unrealistic curves. This analytical model can be used as a first-hand approximation which can facilitate the design of the fiber concrete material required for a specific purpose. Predicting the entire compressive properties solely from the knowledge of the material properties like matrix strength, fiber volume and length is made possible by this modelling. Likewise, the interrelationship and the effect of combination of different material parameters can be examined and simulated using the analytical model.

CONCLUSION

The following conclusion can be drawn from this experimental study related to the stress-strain behavior of coir fiber cement composite under axial compression:

1. The presence of coir fiber altered the morphology of failure during compression, that is gradual failure occurred in spite of the presence of propagating vertical cracks which ultimately maintained the structural integrity of the material.

2. Addition of coir fibers at low volume fraction (Vf, $< 2.0\%$) to cement mortar or concrete did not significantly alter the compressive strength and modulus of elasticity of composite. However, inclusion of fiber in excess of 2% may result to a significant decrease in both strength and elastic modulus.

3. Significant improvement in peak strain, inflection stress and strain and residual load occurred due to coir fiber reinforcement. Thus indicating an enhanced ductility and energy absorption capability of the composite.

4. Linear relationship derived between fiber-matrix parameters and stress-strain relationship can sufficiently predict the properties of natural fiber composite.

5. Analytic expression proposed by Sargin can satisfactorily generate the entire stress-strain curve of coir fiber cement mortar or concrete. This model can effectively estimate the stress-strain properties of a fiber composite material based on the knowledge of compressive strength of matrix or plain mortar/concrete (σm) and fiber parameters such as length (lf), volume (Vf) and elasticity (Ef).

ACKNOWLEDGMENT

The authors wish to thank the support and the assistance of the staff of the Civil Engineering Department of the Integrated Research and Training Center of the Technological University of the Philippines especially Messrs. Rogelio Irabon and Mario Martinez.

REFERENCES

ACI Committee 318 (1989). Building Code Requirement for Reinforced Concrete (ACI 318-83), American Concrete Institute, Detroit, 111 pp.

Akihama, S., Suenaga, T and Banno, T. (1986). Mechanical Properties of Carbon Fiber Reinforced Cement Composites, International Journal of Cement Composites and Lightweight Concrete, Vol. 8 No. 1 Feb. 1986., pp. 21-33.

Carreira, D, and Chu, K.H. (1985). Stress-strain Relationship for Plain Concrete in Compression, ACI Journal Nov. Dec. 1985. ACI, USA pp. 797-803

Dardare, J., Contribution a l'etude Du Comportement Mecanique des Betons Renforces Avec des Fibres de Polypropylene, Composites, Testing, Standards and Design, pp. 227-235.

Desayi, P. and Krishnan, S. (1969). Equation for Stress-strain Curve of Concrete, ACI Journal Proceeding 61, March 1969. pp.345-350.

Fanella, D. and Naaman, A.E. (1985). Stress-strain Properties of Fiber Reinforced Mortar in Compression, ACI Journal, July 1985, ACI USA pp. 475-483.

Gopalaratnam, V.S. and Shah, S.P. (1987). Tensile Failure of Steel Fiber Reinforced Mortar, ASCE, Journal of Engineering Material, Vol. 113, No. 5, May 1987, USA. pp. 635-652.

Gram, H.E. (1984). Durability of Natural Fibers in Concrete, SAREC Report R-2, Sweden, pp.65-100.

Hognestad, E.H., and Hanson, N.W. and McHenry, D. (1995). Concrete Stress Distribution in Ultimate Strength Design, ACI Journal, Dec. 1955, ACI, USA pp. 455-480.

Hussin, M. W. and Zakaria, F.(1990). Prospects for Coconut Fiber Reinforced Thin Cement Sheets in the Malaysian Construction Industry, Proc. 2nd RILEM International Symposium on the Vegetable Plants and their Fiber as Building Materials. Ed. H.S. Sobral, Brazil 1990 pp. 77-86.

JCI (Japan Concrete Institute) (1984). JCI Standards for Test Method of Fiber Reinforced Concrete, JCI-SF, Tokyo, 1984 pp.34-68.

Jorillo, P.A. and Shimizu, G. (1991). Fresh and Mechanical Properties of Discrete Short Coir Fibers in Cement Based Mortar Matrix, Proc. of CONET 91, International Conference on Concrete Eng. and Tech., Kuala Lumpur, Malaysia, pp. 3-13 to 3-26.

Jorillo, P.A. and Shimizu G. (1992). Coir Fiber Reinforced Cement Based Composite, Proc, of 4th RILEM International Symposium on Fiber Cement and Concrete, Sheffield, England, pp. 1096-1106.

Jorillo, P.A. (1994). Properties of Lightweight Gypsum Based Fiber Composite. Microstructure and Flexural Properties, Philippine Industrial Education and Technology.

Jorillo, P.A., Suzuki, T., and Murayama, Y. (1993). Qualitative Testing of Fiber Centrifugated Concrete, Nihon University Research Presentation.

Kris, L.B., and Lee, S.L. (1960). Ultimate Strength of Over Reinforced Beam. Proceeding ASCE V. 86 June 1960, pp. 95-105.

Popovics, S. (1973). Numerical Approach to the Complete Stress-strain Curve of Concrete, Cement and Concrete Research. Vol. 3, pp. 583-599.

Rush H. and Sell, R. (1961). Deutscher Ausschuss Fur Stahlbeton, Heft 143, Berlin.

Sargin, M. (1971). Stress-strain Relationship for Concrete and the Analysis of Structural Concrete Cross Sections, Study No. 4 Solid Mechanics Division, University of Waterloo, pp. 210.

Schaffner, B. Preparation of Coir Fiber from Coconut Husk, FCR News Swiss Center for Appropriate Technology, Switzerland, pp. 10-11.

Swamy, R.N. Fiber Reinforcement of Cement and Concrete: 19-FRC Committee, Materials and Structures Vol. 8, No. 45, France, pp 235-255.

Swamy, R.N. (1990). Vegetable Fiber Reinforced Cement Composites a False Dream or a Potential Reality?, 2nd RILEM International Symposium on Vegetable Plants and their Fibers as Building Materials, Ed. Sobral, Brazil, pp. 3-8.

Walkus, B.R. Junskiewicz A. and Jeruzal, J. (1979). Concrete Composites with Cut Steel Fiber Reinforcement Subjected to Uniaxial Tension, ACI Materials Journal, Oct. 1979 ACI, USA, pp. 1070-1092.

Wang, P.T., Shah, S.P. and Naaman, A.E. (1978). Stress-strain Curves of Normal and Lightweight Concrete in Compression, ACI Journal, Nov. 1978, ACI, USA, pp. 603-611.

Ward, R.J., and Li, V.C. (1990). Dependence of Flexural Behavior of Fiber Reinforced Mortar in Material Fracture Resistance and Beam Size, ACI Materials Journal Nov.-Dec. 1990, ACI USA, pp. 627-637.

Table 5
Compressive strength properties of concrete and mortar-based composites

Mix code	Fiber volume (%)	Comp. Strength (kgf/cm^2)	Coeff of Variation (%)	Peak Strain ($\mu\varepsilon$)	Elastic Modulus (kgf/cm^2)	nflection Stress (kgf/cm^2)	Inflection Strain ($\mu\varepsilon$)	Last Point Stress (kgf/cm^2)
Concrete 3C40 Series w/c = 40 lf = 30	0.0	440	122	1812	321,000	undefined	undefined	undefined
	0.5	481	9.1	2132	333,200	330	3057	80
	1.0	448	9.3	1887	307,300	347	2462	80
	2.0	438	5.0	1900	267,000	240	2200	76
	3.0	380	10.0	2600	213,800	260	3500	86
Concrete 3C50 Series w/c = 50 lf = 30	0.0	362	8.6	1743	283,300	undefined	undefined	undefined
	1.0	353	8.7	1900	299,300	226	3193	72
	2.0	377	4.9	1888	276,800	265	2416	49
	3.0	343	9.2	2025	235,100	233	4167	110
Concrete 3C50 Series w/c = 60 lf = 30	0.0	283	10..3	1320	280,300	undefined	undefined	undefined
	0.5	299	8.6	1725	270,600	265	2000	86
	1.0	256	8.9	1550	259,700	230	2075	75
	2.0	254	7.2	2392	228,100	210	4750	110
	3.0	298	2.0	2775	179,300	248	3475	96
Mortar 1M50 Series w/c = 50 lf = 10	0.0	434	5.8	2180	259,700	undefined	undefined	undefined
	0.5	410	3.7	2417	235,700	280	2800	60
	2.0	381	5.1	2200	228,200	280	3125	80
	3.0	348	8.6	2800	208,900	292	4350	112
3M50 Series w/c = 50 lf = 30	0.5	464	6.8	2850	232,000	280	3100	80
	2.0	336	8.3	1750	232,600	280	2200	60
	3.0	344	7.6	2350	221,100	292	3500	70
6M50 Series w/c = 50 lf = 60	0.5	434	2.3	2625	237,500	328	2900	76
	2.0	312	9.3	2000	216,000	240	2200	80
	3.0	380	10.2	2600	213,800	260	3500	116
3M50 Series w/c = 50 lf = 30	0.0	354	11.5	2360	228,300	undefined	undefined	undefined
	0.5	364	1.1	2650	204,800	298	2875	60
	2.0	304	5.3	2450	182,600	258	3000	62

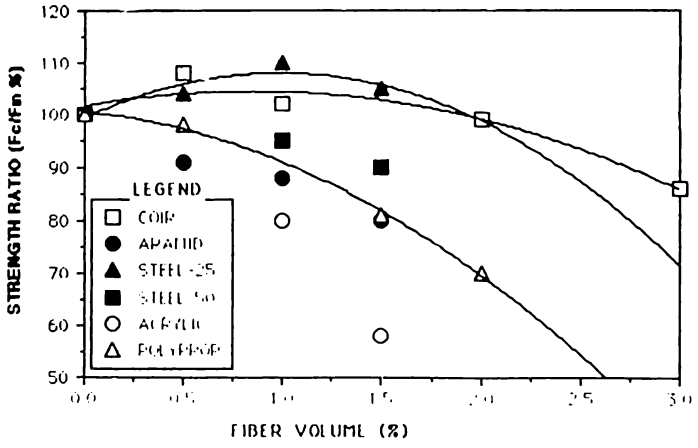

Figure 3(a)
Trend of Compressive strength of various fiber concrete

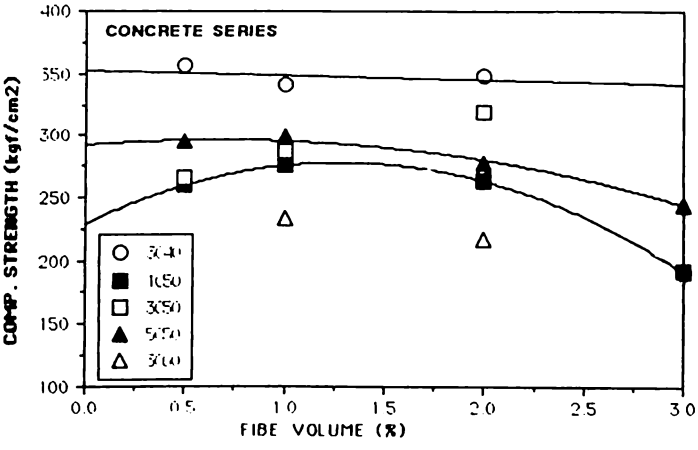

Figure 3(b)
Trend of Compressive strength of coir fiber concrete at 28 days

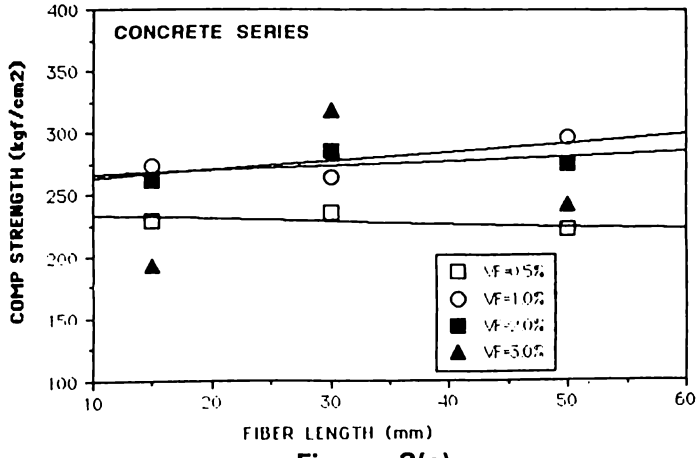

Figure 3(c)
Effect of fiber length to compressive strength of coir fiber concrete

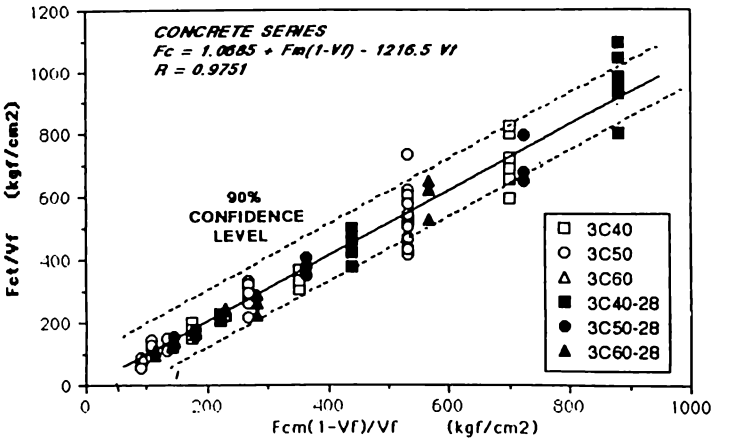

Figure 4
Correlation of compressive strength and fiber-matrix parameters

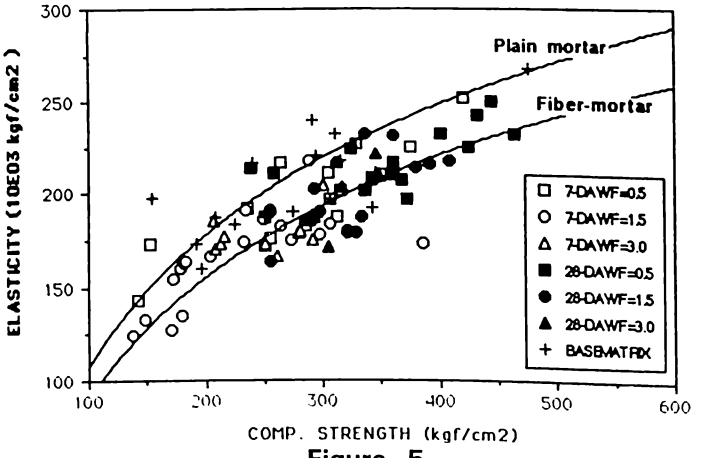

Figure 5
Relationship of comp. strength and elastic modulus for Mortar series

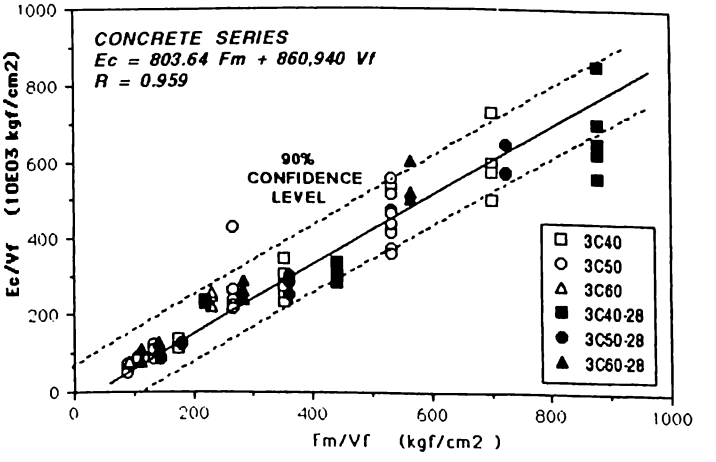

Figure 6
Correlation of Elastic modulus and matrix-fiber parameters

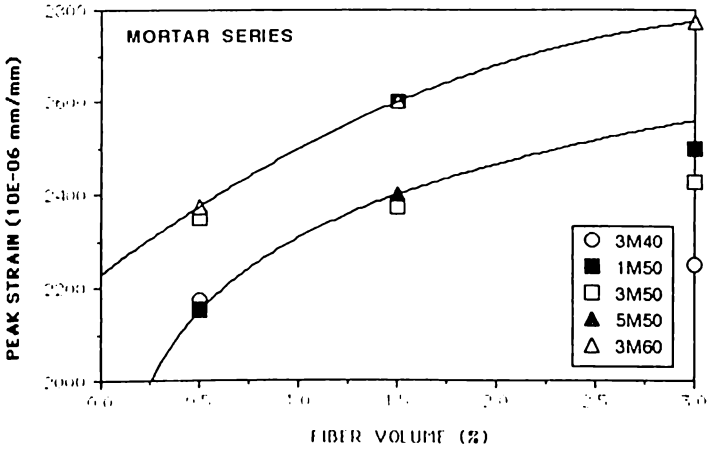

Figure 7(a)

Effect of fiber volume to peak strain

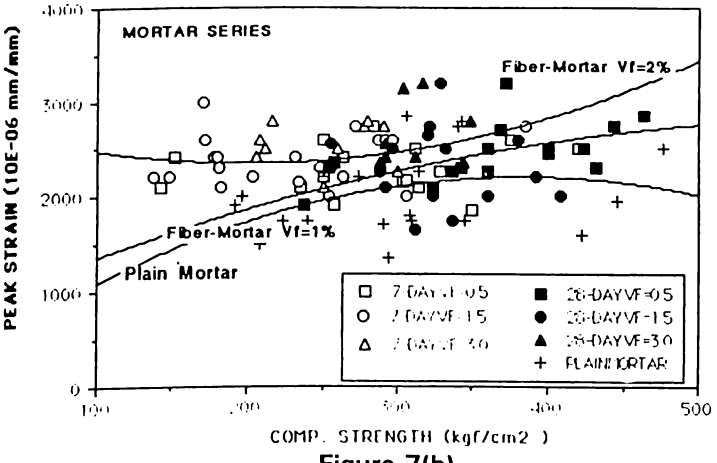

Figure 7(b)

Relationship of compressive strength and peak strain of coir fiber composite

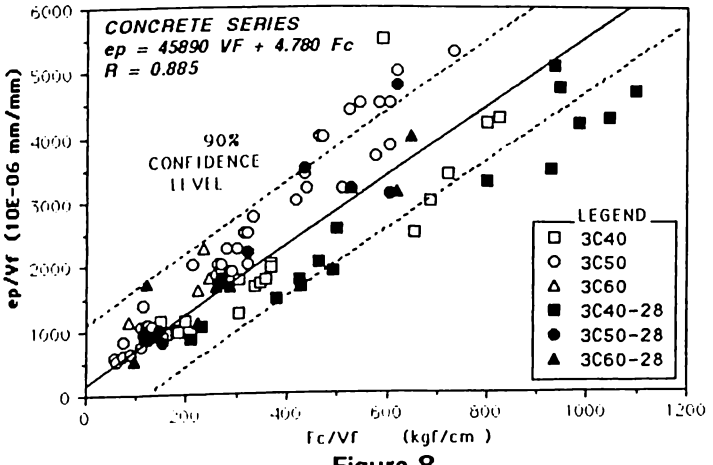

Figure 8

Correlation of peak strain with fiber- matrix parameters

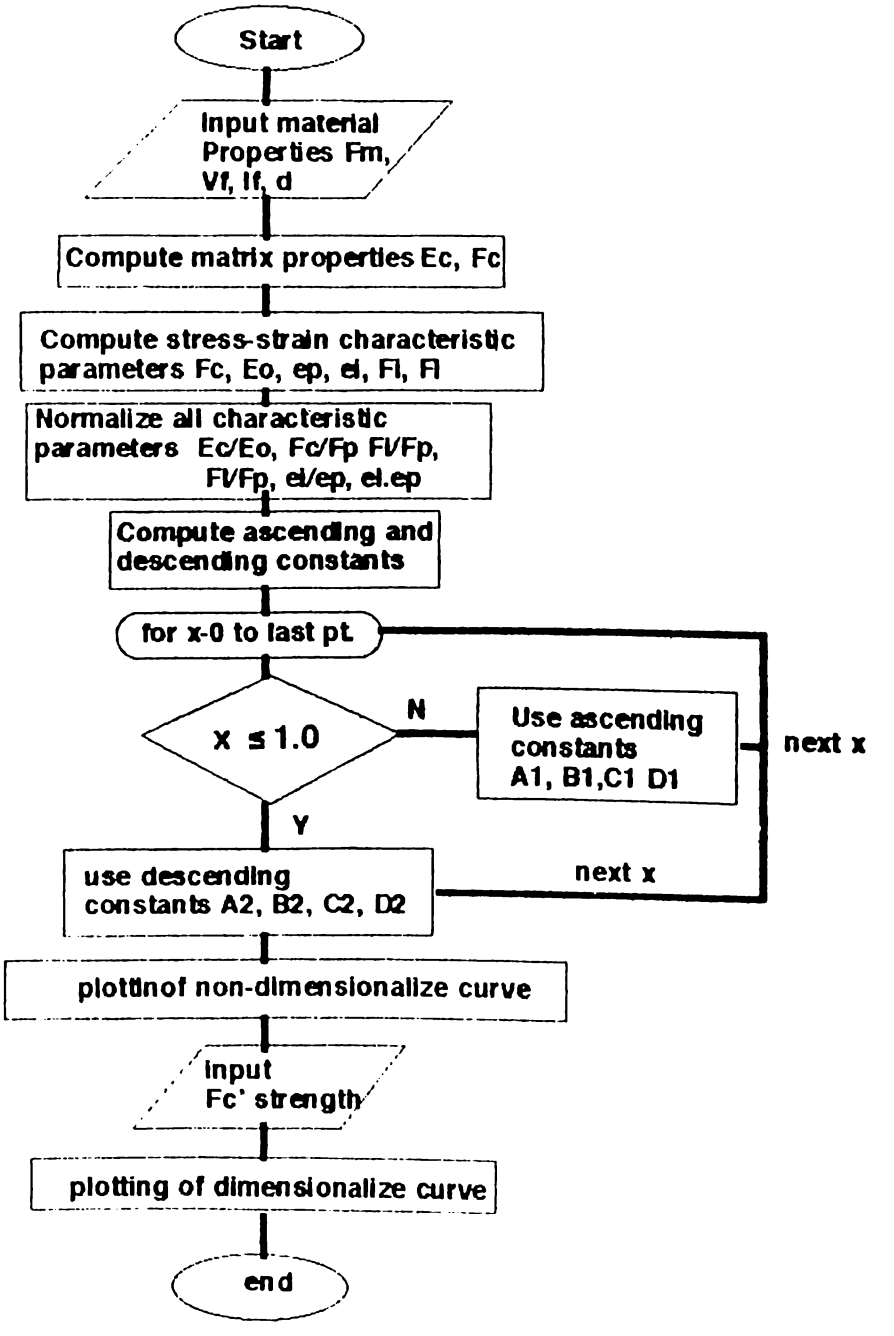

Figure 9
Flowchart of Analytical generation of Stree-strain curve

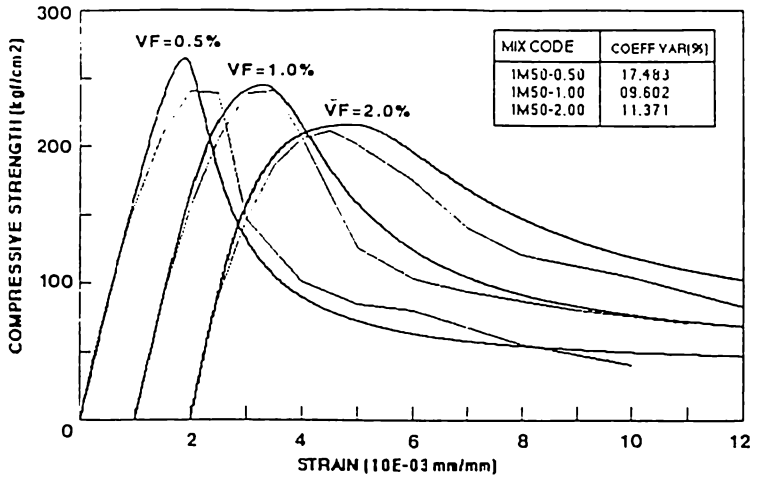

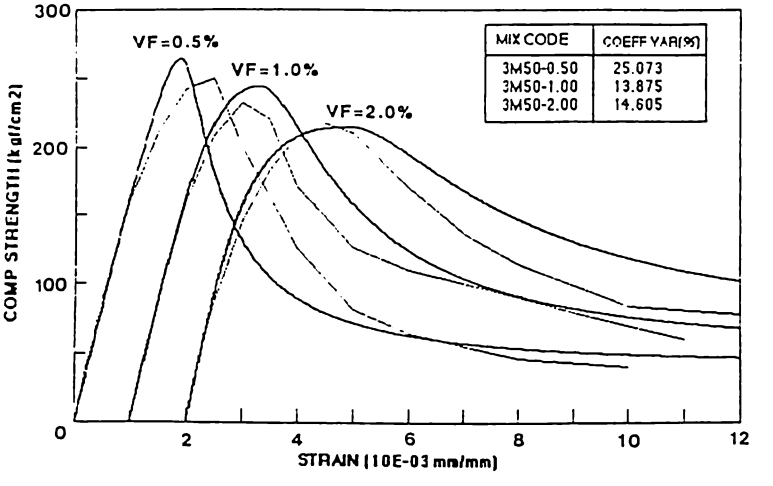

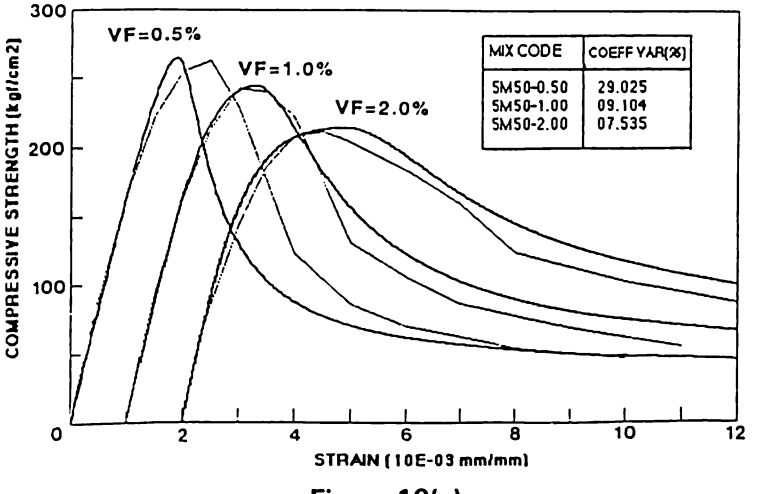

Figure 10(a)
Comparison of the Analytically generated curve and the experimental stress-strain curve for Mortar series

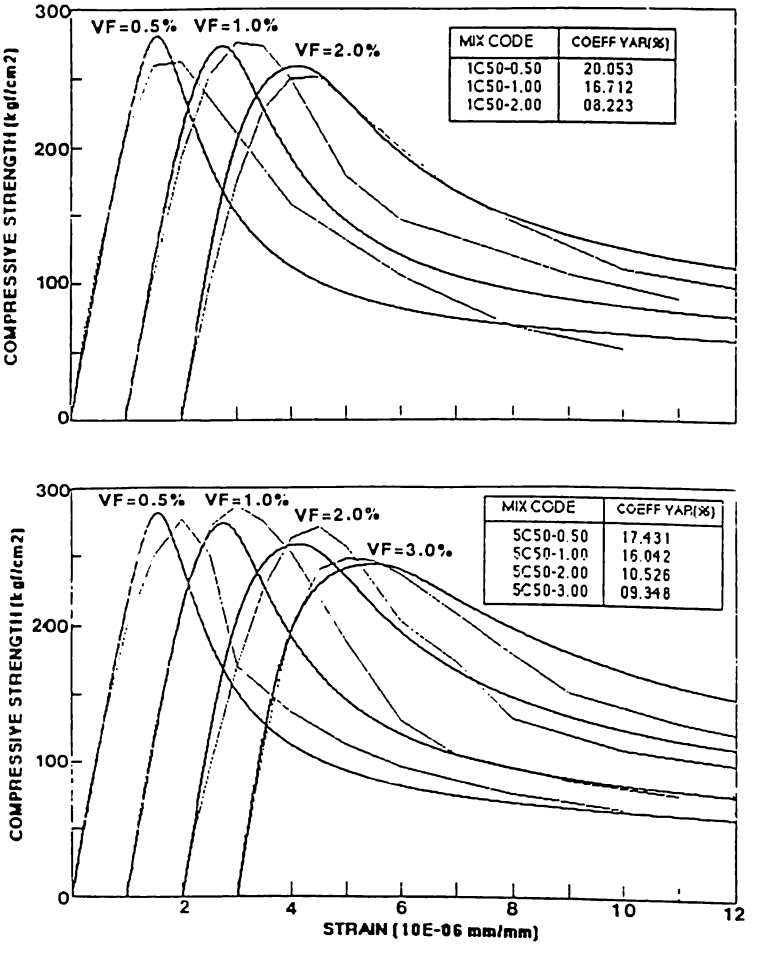

Figure 10(b)
Comparison of the Analytically generated curve and the experimental stress-strain curve for concrete series